

Electronic Supplementary Information

The Nature of Excited States in Dipolar Donor/Fullerene Complexes for Organic Solar Cells: Evolution with the Donor Stack Size

Xingxing Shen,^{1,2} Guangchao Han,^{1,2} Yuanping Yi^{1,}*

¹Beijing National Laboratory for Molecular Sciences, CAS Key Laboratory of
Organic Solids, Institute of Chemistry, Chinese Academy of Sciences, Beijing 100190,
China

²University of Chinese Academy Sciences, Beijing 100049, China

Contents

Figure S1. (a) Chemical structures of DTDCTB and C₆₀ and (b) Illustrations of the two kinds of cofacial intermolecular π - π stacking (I and II) in DTDCTB crystal and donor-acceptor interfacial geometry (DA_{CC} and DA_H).

Figure S2. Natural transition orbitals of (a) the lowest *dd*CT state and (b) the lowest dark EX state in DTDCTB clusters.

Figure S3. The frontier molecular orbitals of *n*DTDCTB/C_{60CC} complexes.

Figure S4. The structures (a) and frontier molecular orbitals (b) of *n*DTDCTB/C_{60H} complexes.

Figure S5. Energy levels of frontier molecular orbitals and IP and EA values for the *n*DTDCTB/C_{60H} complexes.

Figure S6. Energy level of (a) the EX states and the *dd*CT states between adjacent DTDCTB molecules and (b) donor-to-acceptor CT states in *n*DTDCTB/C_{60H} complexes.

Figure S7. The oscillator strengths of the lowest bright EX states in complexes.

Figure S8. Natural transition orbitals of the lowest EX state with a large oscillator strength in *n*DTDCTB/C_{60H} complexes.

Figure S9. Natural transition orbitals of the lowest dark EX states of (a) *n*DTDCTB/C_{60CC} and (b) *n*DTDCTB/C_{60H} complexes.

Figure S10. Natural transition orbitals of the lowest *dd*CT states of (a) *n*DTDCTB/C_{60CC} and (b) *n*DTDCTB/C_{60H} complexes.

Figure S11. Natural transition orbitals of the lowest α CT, β CT, γ CT states in (a) 1~3DTDCTB/C_{60CC} and (b) 1~3DTDCTB/C_{60H} complexes.

Figure S12. Natural transition orbitals of the lowest α CT, β CT, γ CT, δ CT states in complex 4DTDCTB/C_{60H}.

Table S1. The electronic couplings for hole transfer, electron transfer and charge recombination, and binding energies for dimers I, II, DA_{CC}, and DA_H calculated by DFT using the B3LYP and tuned- ω B97X functionals with different basis sets.

Table S2. The optimized range-separation parameters of DTDCTB clusters and *n*DTDCTB/C₆₀ complexes.

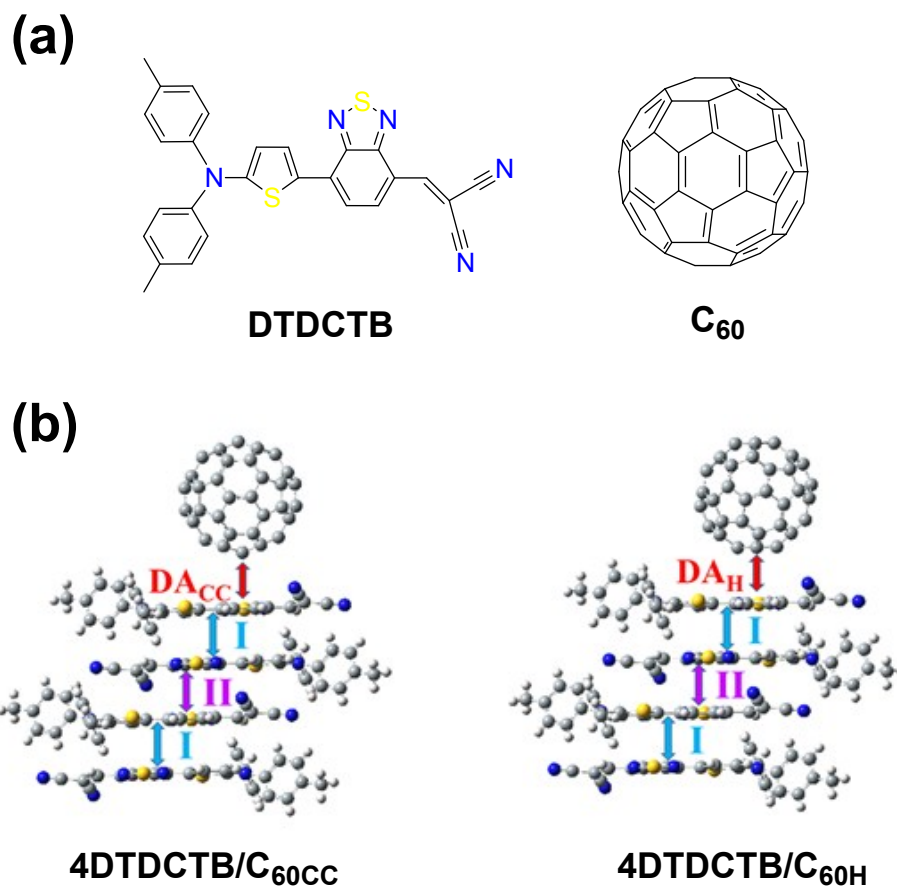


Figure S1. (a) Chemical structures of DTDCTB and C₆₀ and (b) Illustrations of the two kinds of cofacial intermolecular π - π stacking (I and II) in DTDCTB crystal and donor-acceptor interfacial geometry (DA_{CC} and DA_H).

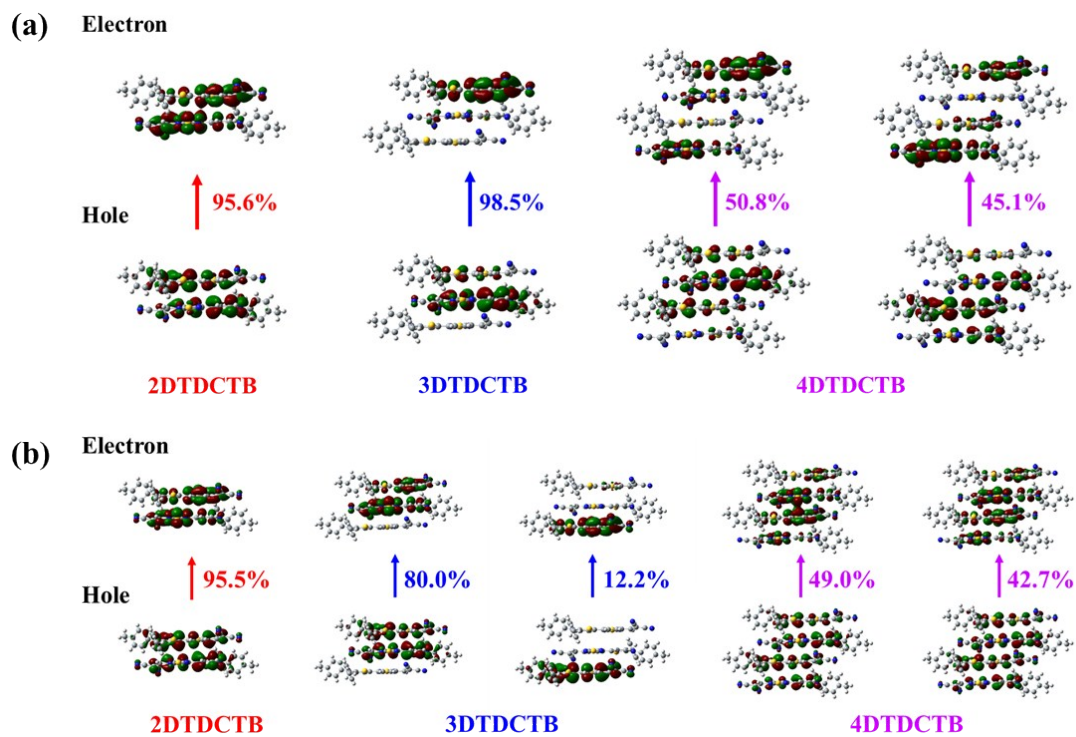


Figure S2. Natural transition orbitals of (a) the lowest *ddCT* state and (b) the lowest dark EX state in DTDCTB clusters. The weight of the hole-electron contribution to the excitation also included.

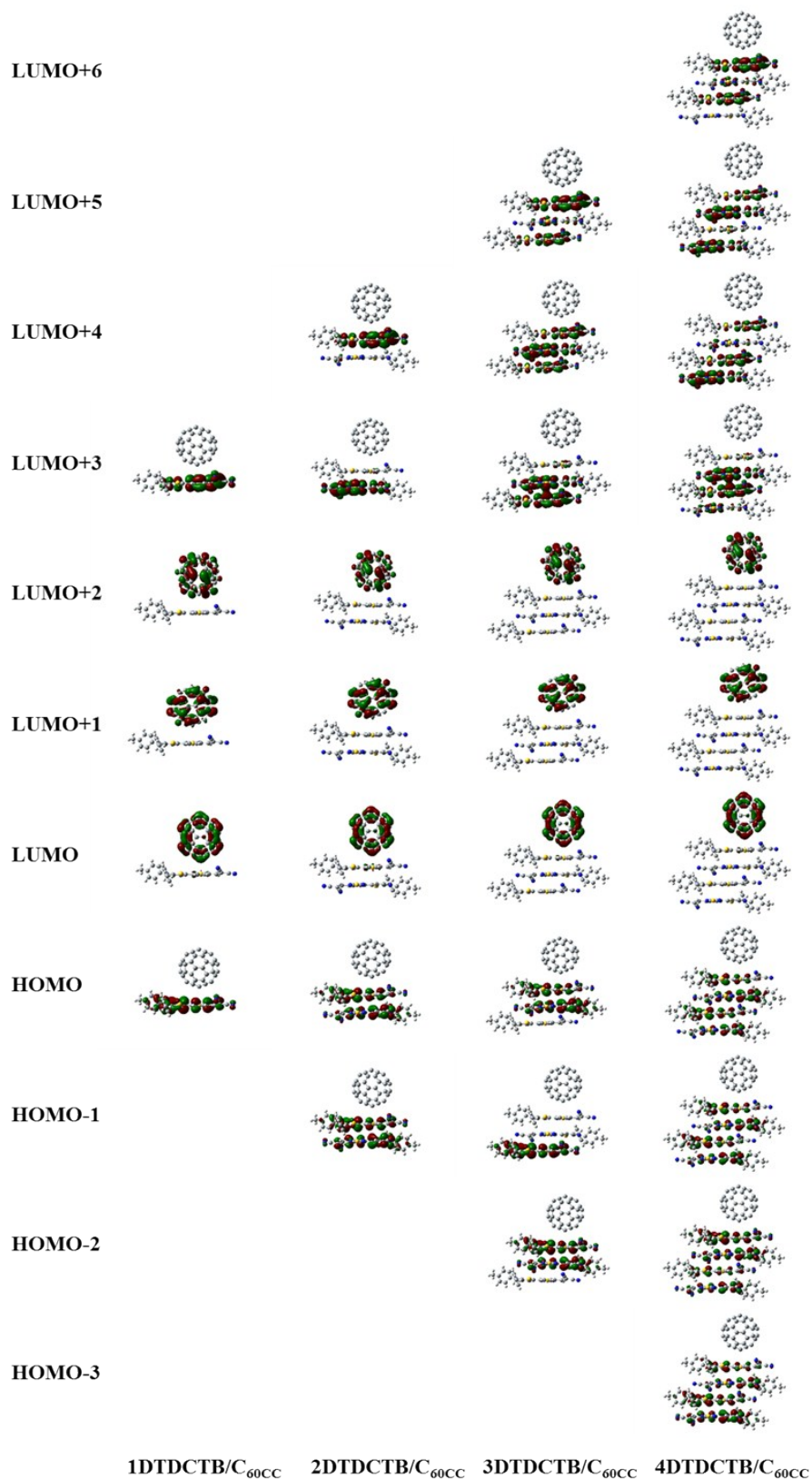


Figure S3. The frontier molecular orbitals of n DTDCTB/C_{60CC} complexes.

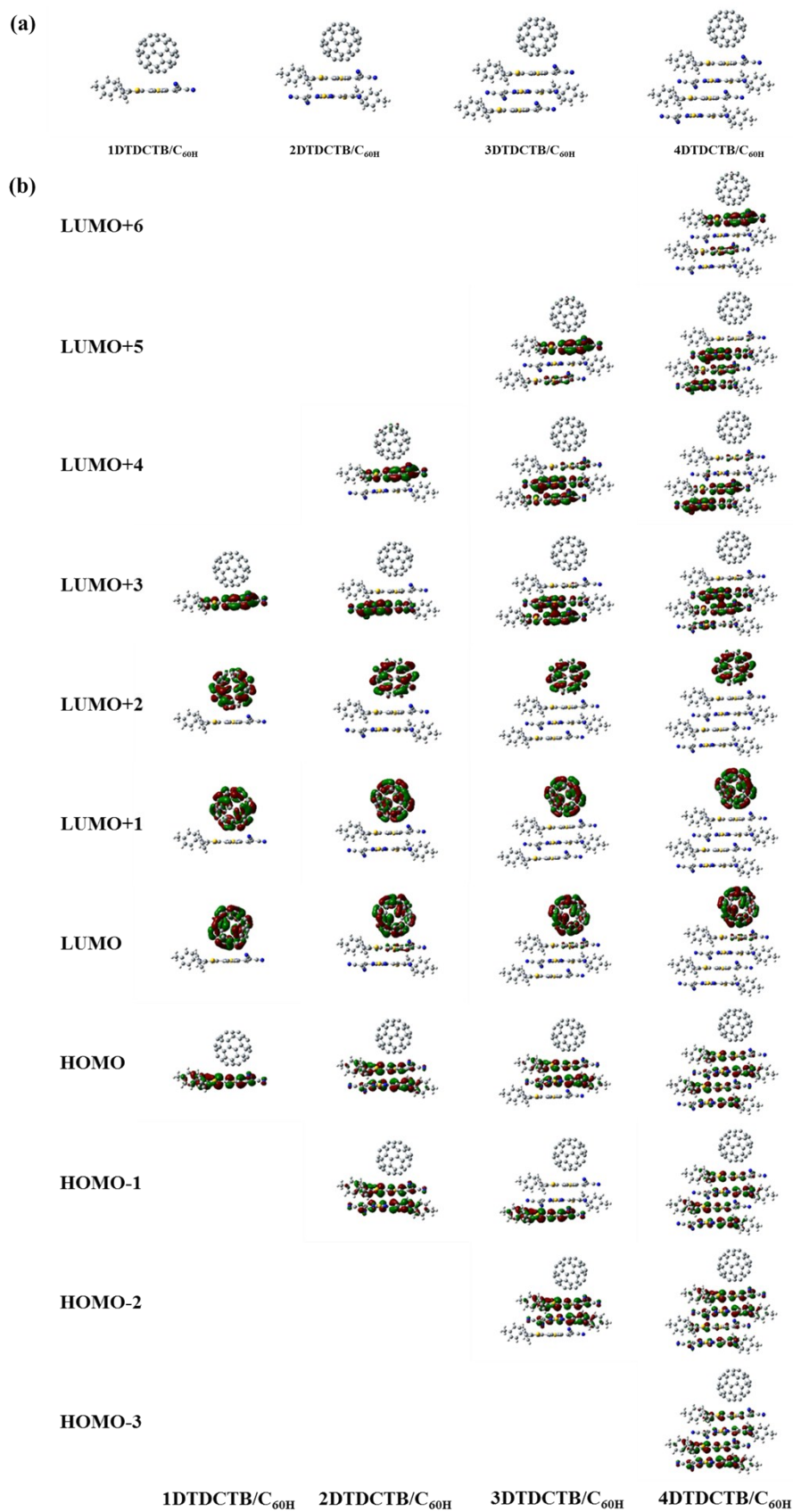


Figure S4. The structures (a) and frontier molecular orbitals (b) of n DTDCTB/C_{60H} complexes.

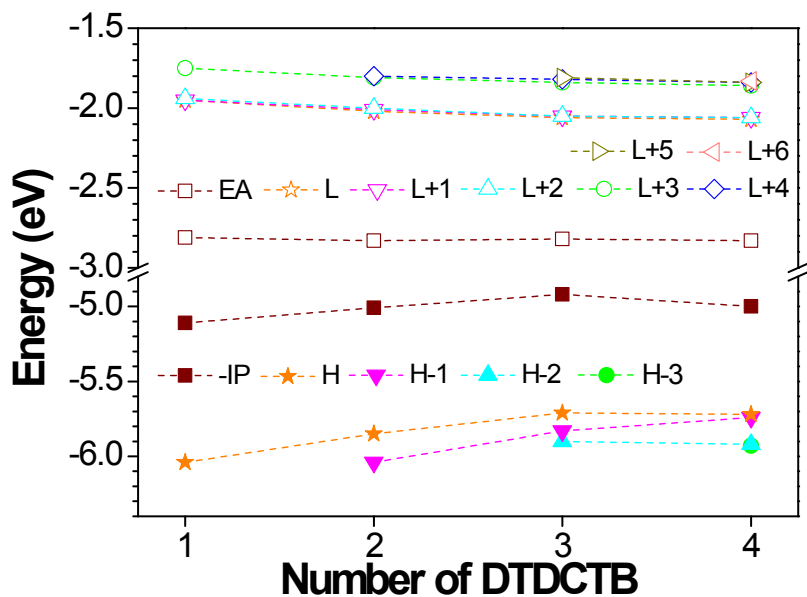


Figure S5. Energy levels of frontier molecular orbitals and IP and EA values for the n DTDCTB/ C_{60H} complexes (H and L denote HOMO and LUMO, respectively).

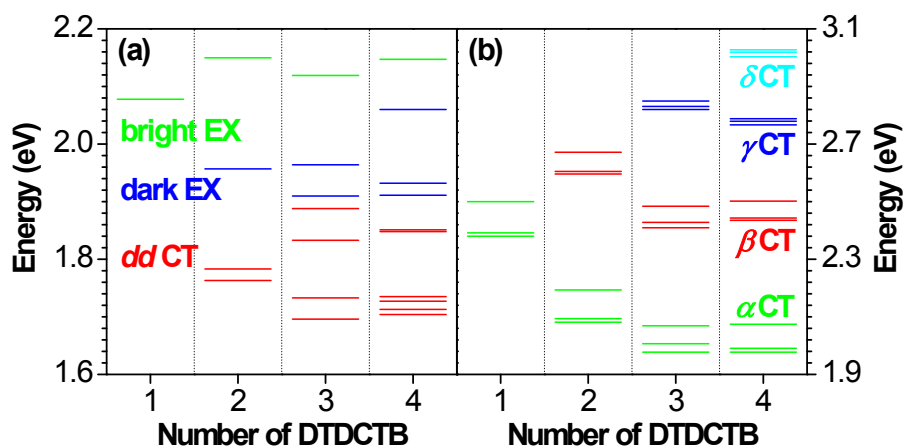


Figure S6. Energy level of (a) the EX states and the $ddCT$ states between adjacent DTDCTB molecules and (b) donor-to-acceptor CT states in n DTDCTB/ C_{60H} complexes.

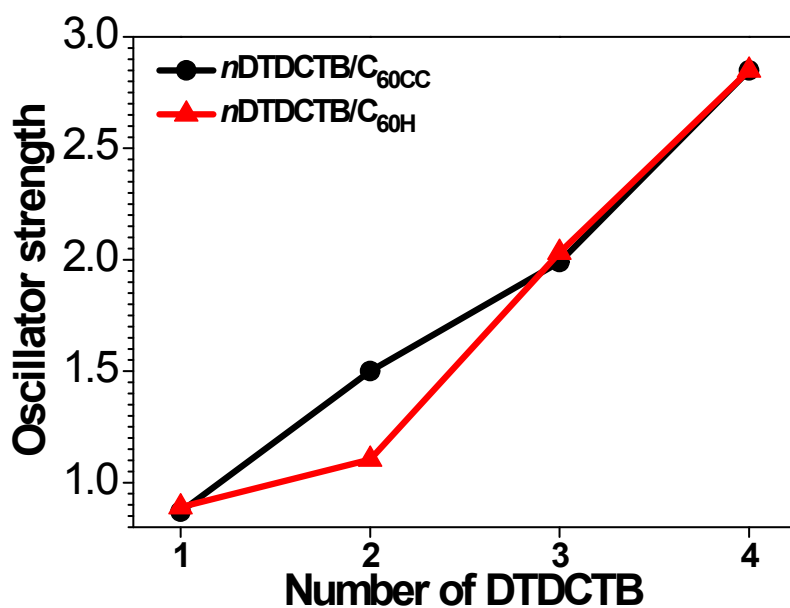


Figure S7. The oscillator strengths of the lowest bright EX states in complexes.

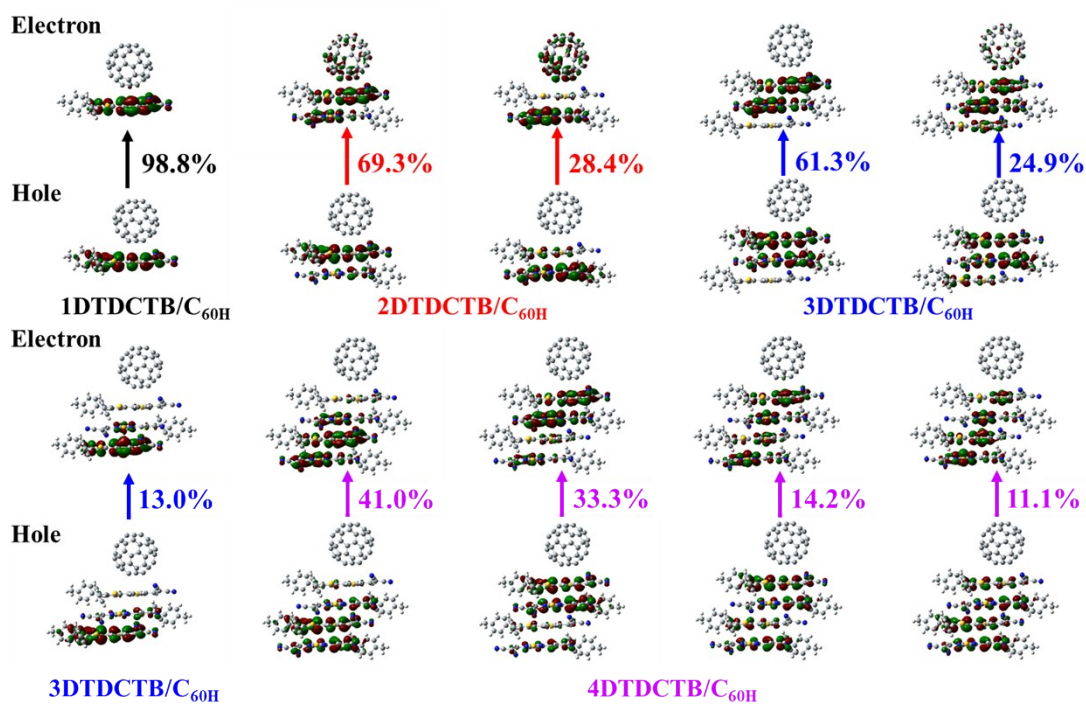


Figure S8. Natural transition orbitals of the lowest EX state with a large oscillator strength in n DTDCTB/ C_{60H} complexes. The weight of the hole-electron contribution to the excitation also included.

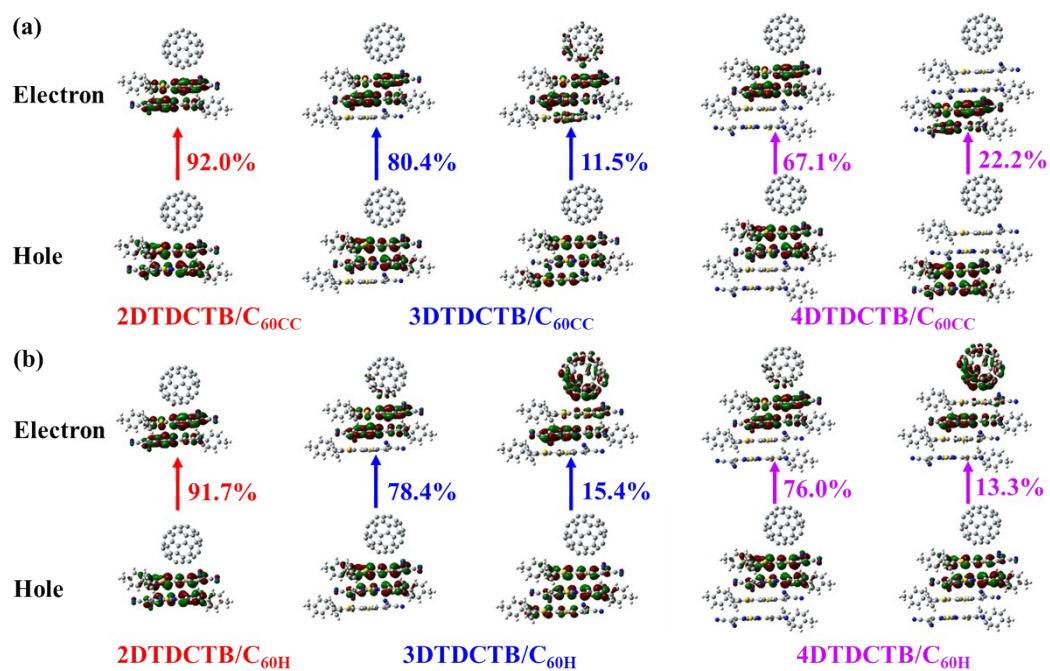


Figure S9. Natural transition orbitals of the lowest dark EX states of (a) n DTDCTB/C_{60CC} and (b) n DTDCTB/C_{60H} complexes. The weight of the hole-electron contribution to the excitation also included.

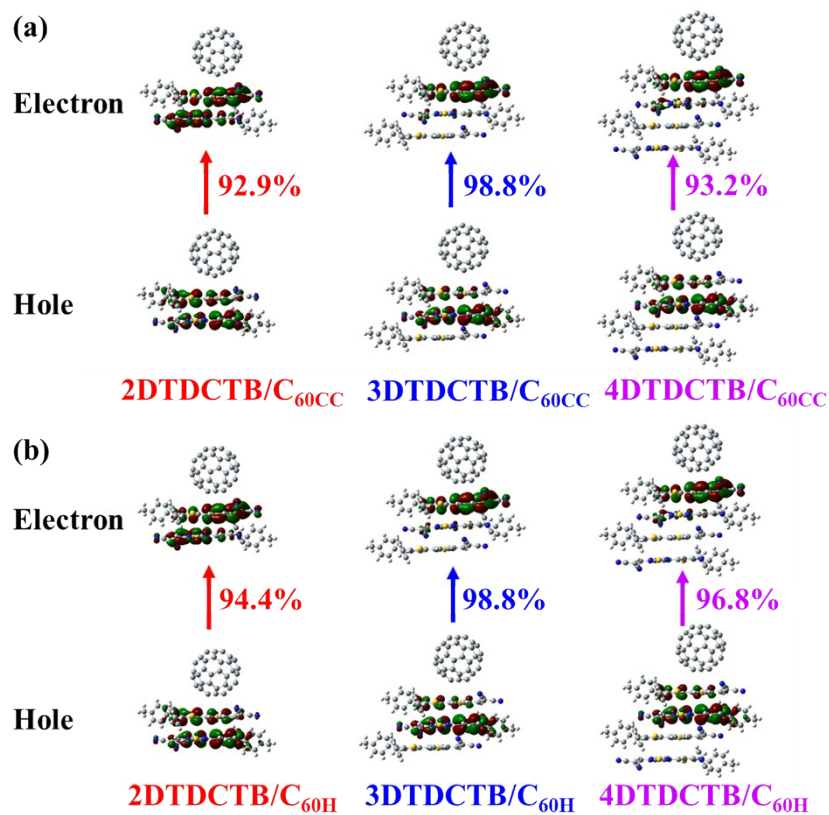


Figure S10. Natural transition orbitals of the lowest dd CT states of (a) n DTDCTB/C_{60CC} and (b) n DTDCTB/C_{60H} complexes. The weight of the hole-electron contribution to the excitation also included.

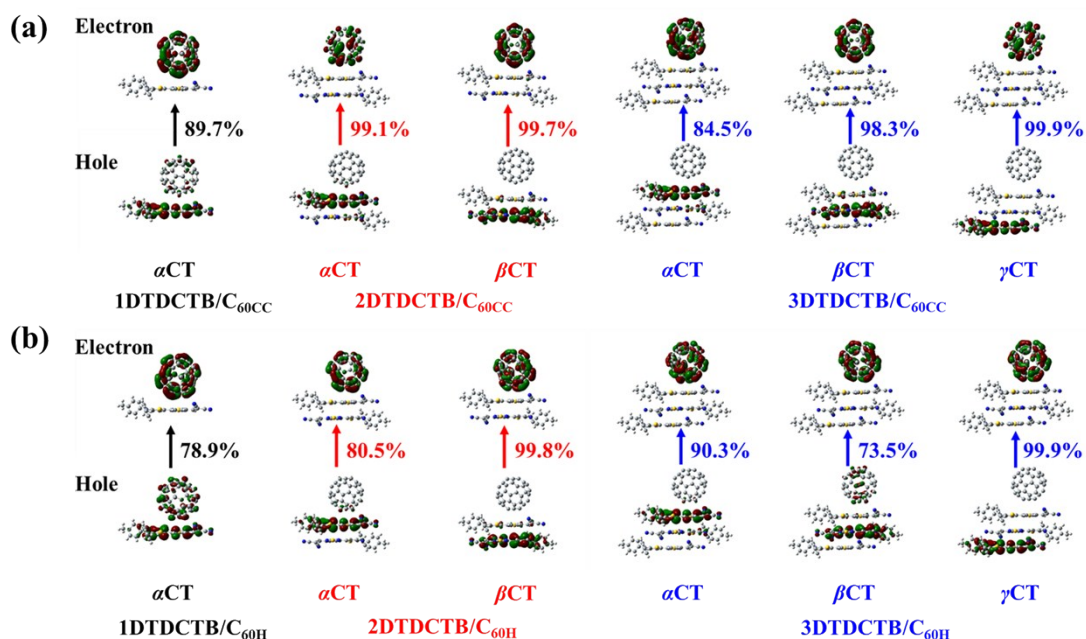


Figure S11. Natural transition orbitals of the lowest α CT, β CT, γ CT states in (a) 1~3DTDCTB/ C_{60CC} and (b) 1~3DTDCTB/ C_{60H} complexes. The weight of the hole-electron contribution to the excitation also included.

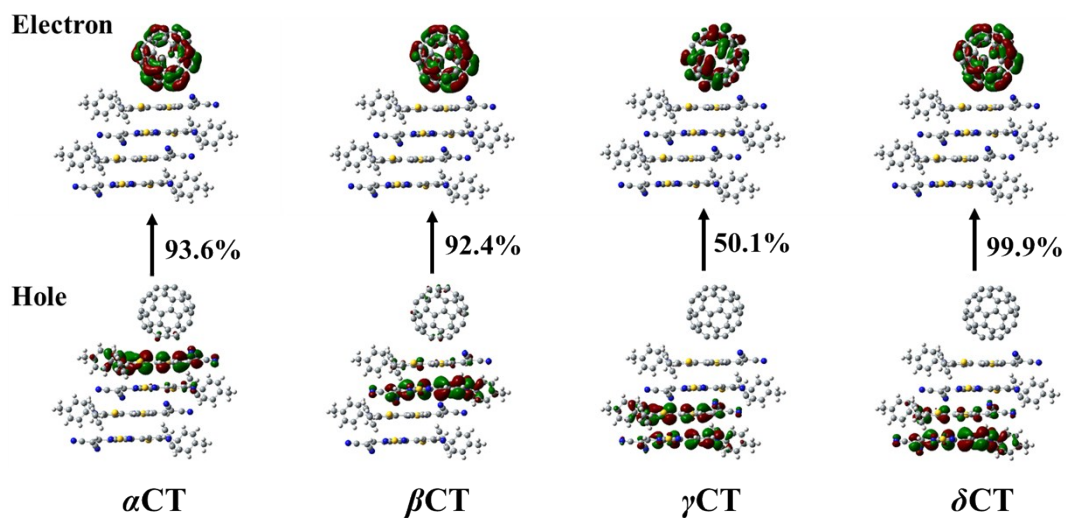


Figure S12. Natural transition orbitals of the lowest α CT, β CT, γ CT, δ CT states in complex 4DTDCTB/ C_{60H} . The weight of the hole-electron contribution to the excitation also included.

Table S1. The electronic couplings (in meV) for hole transfer (t_h), electron transfer (t_e) and charge recombination (t_R), and binding energies (E_b , in kcal/mol) for dimers I, II, DA_{CC} , and DA_H calculated by DFT using the B3LYP and tuned- ω B97X functionals with different basis sets.

B3LYP/(6-31G*, 6-31G**, 6-311G**)				
	t_h	t_e	t_R	E_b
I	79.9, 79.7, 82.9	21.8, 21.2, 21.0	28.3, 29.2, 34.5	-21.2, -21.2, -21.9
II	28.3, 28.5, 29.7	12.7, 12.9, 15.5	25.8, 25.4, 24.6	-20.1, -20.1, -21.0
DA_{CC}	15.4, 15.4, 16.1	36.3, 36.0, 34.1	15.9, 15.8, 16.4	—
DA_H	16.7, 16.7, 16.2	25.2, 25.1, 26.8	40.2, 40.1, 42.5	—
tuned-ωB97X/(6-31G*, 6-31G**, 6-311G**)				
	t_h	t_e	t_R	E_b
I	85.6, 85.3, 88.7	19.3, 18.6, 16.6	54.3, 56.0, 65.5	-20.5, -20.6, -22.1
II	27.9, 28.2, 29.4	4.9, 5.0, 5.5	49.8, 49.1, 49.5	-18.9, -18.9, -21.0
DA_{CC}	16.4, 16.3, 17.6	38.5, 38.2, 37.2	24.8, 24.7, 26.8	—
DA_H	17.7, 17.6, 17.5	29.8, 29.7, 32.4	64.9, 64.7, 70.6	—

^a Considering the degeneracy of HOMO and LUMO in C_{60} , the effective electronic couplings are calculated for DA_{CC} and DA_H .

Table S2. The optimized range-separation parameters (ω) of DTDCTB clusters and nDTDCTB/ C_{60} complexes.

	1DTDCTB	2DTDCTB	3DTDCTB	4DTDCTB
ω	0.14	0.12	0.10	0.10
	1DTDCTB/ C_{60}	2DTDCTB/ C_{60}	3DTDCTB/ C_{60}	4DTDCTB/ C_{60}
ω	0.13	0.11	0.10	0.10